Early biochemical events in insulin-stimulated fluid phase endocytosis

Diana M. Pitterle, Robert T. Sperling, Martin G. Myers, Jr., Morris F. White and Perry J. Blackshear

AJP - Endo 276:94-105, 1999.

AJP - Endocrinology and Metabolism publishes results of original studies about endocrine and metabolic systems on any level of organization. It is published 12 times a year (monthly) by the American Physiological Society, 9650 Rockville Pike, Bethesda MD 20814-3991. ISSN: 0193-1849, ESSN: 1522-1555. Visit our website at http://www.the-aps.org/.

American Journal of Physiology – Endocrinology and Metabolism

Early biochemical events in insulin-stimulated fluid phase endocytosis

DIANA M. PITTERLE,[1] ROBERT T. SPERLING,[2] MARTIN G. MYERS, JR.,[3] MORRIS F. WHITE,[3] AND PERRY J. BLACKSHEAR[1,4]

[1]*Departments of Medicine and Biochemistry, Duke University Medical Center, Durham 27710;* [4]*Office of Clinical Research and Laboratory of Signal Transduction, National Institute of Environmental Health Sciences, Research Triangle Park, North Carolina 27709;* [2]*Department of Medicine, Brigham and Women's Hospital, Boston 02115; and* [3]*Research Division, Joslin Diabetes Center, Department of Medicine and Program in Cell and Developmental Biology, Harvard Medical School, Boston, Massachusetts 02215*

Pitterle, Diana M., Robert T. Sperling, Martin G. Myers, Jr., Morris F. White, and Perry J. Blackshear. Early biochemical events in insulin-stimulated fluid phase endocytosis. *Am. J. Physiol.* 276 (*Endocrinol. Metab.* 39): E94–E105, 1999.—We examined the initial molecular mechanisms by which cells nonselectively internalize extracellular solutes in response to insulin. Insulin-stimulated fluid phase endocytosis (FPE) was examined in responsive cells, and the roles of the insulin receptor, insulin receptor substrate-1 (IRS-1), phosphatidylinositol 3′-kinase (PI 3′-kinase), Ras, and mitogen-activated protein kinase kinase (MEK) were assessed. Active insulin receptors were essential, as demonstrated by the stimulation of FPE by insulin in HIRc-B cells (Rat-1 cells expressing 1.2×10^6 normal insulin receptors/cell) but not in untransfected Rat-1 cells or in Rat-1 cells expressing the inactive A/K1018 receptor. IRS-1 expression augmented insulin-stimulated FPE, as assessed in 32D cells, a hematopoietic precursor cell line lacking endogenous IRS-1. Insulin-stimulated FPE was inhibited in mouse brown adipose tissue (BAT) cells expressing the 17N dominant negative mutant Ras and was augmented in cells expressing wild-type Ras. The MEK inhibitor PD-98059 had little effect on insulin-stimulated FPE in BAT cells. In 32D cells, but not in HIRc-B and BAT cells, insulin-stimulated FPE was inhibited by 10 nM wortmannin, an inhibitor of PI 3′-kinase. The results indicate that the insulin receptor, IRS-1, Ras, and, perhaps in certain cell types, PI 3′-kinase are involved in mediating insulin-stimulated FPE.

pinocytosis; signaling pathways; wortmannin; PD-98059; horseradish peroxidase

INSULIN ELICITS both metabolic and mitogenic responses in cells expressing its receptor, and recent studies suggest that these responses are likely to be mediated though separate intracellular signaling pathways (32, 45, 56). Metabolic responses include rapid increases in the cellular uptake and storage of glucose, lipids, and amino acids and the inhibition of cellular processes that release these molecules in the bloodstream. The biochemical mechanisms that mediate many of these acute metabolic effects of insulin remain poorly understood.

In contrast, the growth-promoting or mitogenic effects of insulin appear to involve many of the pathways utilized by other growth factors whose receptors have intrinsic tyrosine kinase activity (47). Common features include *1*) activation of the intrinsic tyrosine kinase activity of the receptor on binding of the growth factor; *2*) autophosphorylation of the receptor on tyrosine residues; *3*) activation of phosphatidylinositol 3′-kinase (PI 3′-kinase); *4*) activation of Ras; and *5*) activation of the mitogen-activated protein kinase (MAP kinase) cascade. For most receptor protein tyrosine kinases, the phosphotyrosines generated within their receptors become binding sites for the src-homology 2 domains of proteins such as PI 3′-kinase and the GRB2/son of sevenless (SOS) or GRB2/Shc complexes that can activate Ras (53).

Although the insulin receptor contains phosphotyrosines that may be bound in a similar fashion, the primary signaling pathway is mediated through receptor phosphorylation of a large intracellular protein, insulin receptor substrate-1 (IRS-1), on tyrosines; the activation of PI 3′-kinase and Ras occurs when PI 3′-kinase and the GRB2/SOS complex bind to the phosphotyrosines in IRS-1. In addition, several other proteins have been shown to bind to the phosphotyrosines in IRS-1, including the tyrosine phosphatase Syp and the cytoplasmic tyrosine kinase Nck. Many of the available data indicate that phosphorylated IRS-1 acts as the scaffold upon which an insulin-dependent signaling complex is built (reviewed in Ref. 36).

Insulin and other growth factors have another feature in common: in cells that express their receptors, they stimulate a rapid increase in ruffling and fluid phase endocytosis (FPE; reviewed in Ref. 42). In the case of insulin, internalization of fluid phase vesicles is one of at least four different vesicular trafficking events that occur in response to the hormone, the others being the internalization of the insulin receptor in clathrin-coated vesicles, the recruitment of the intracellular vesicles carrying the glucose transporter to the plasma membrane, and the increase in caveolae at the plasma membrane (4, 6, 46). Each of these vesicular trafficking events occurs within minutes of receptor occupancy by insulin.

The term FPE describes the nonspecific internalization of extracellular fluid in large vesicles derived from the plasma membrane of cells. Addition of sol-

The costs of publication of this article were defrayed in part by the payment of page charges. The article must therefore be hereby marked "*advertisement*" in accordance with 18 U.S.C. Section 1734 solely to indicate this fact.

uble markers such as horseradish peroxidase (HRP), [^{14}C]sucrose, or fluorescent dextran to the extracellular fluid permits this process to be measured (39, 58). FPE is distinguished from receptor-mediated endocytosis by a variety of criteria: *1*) FPE is inhibited by amiloride, a reagent that inhibits the Na^+/H^+ exchanger (55); *2*) fluid phase vesicles are not limited by the size constraints imposed by a clathrin coat as are the vesicles for receptor-mediated endocytosis (43); and *3*) FPE increases linearly with marker concentration and incubation time while receptor-mediated endocytosis is a saturable process (58). Like other forms of endocytosis, FPE is inhibited at 4°C.

A variety of physiological roles have been proposed for growth factor-stimulated FPE, including *1*) nutrient uptake, *2*) removal of insulin and other compounds from the immediate extracellular space, *3*) downregulation of receptors, *4*) plasma membrane turnover, *5*) uptake of extracellular components for subsequent presentation to immunological cells, and *6*) rapid readjustment of intracellular ion concentrations (2, 25, 27, 57, 59). Although the actual physiological functions of this response have not been identified, it is likely that they will vary depending on the type of cell in question. In addition, insulin-stimulated FPE may simply be a by-product of other responses such as plasma membrane ruffling (5) or cell motility (49). Establishing the signaling molecules involved in the pathways from the receptor to these responses (ruffling, FPE, motility) will ultimately allow a determination of their identity or distinctness. To learn more about the mechanism of insulin-stimulated FPE, we have studied this process in a variety of insulin-responsive cell lines using various biochemical tools to assess the involvement of the insulin receptor tyrosine kinase, IRS-1, PI 3′-kinase, Ras, and the MAP kinase cascade. Our results indicate that the insulin receptor, IRS-1, and Ras are involved in mediating insulin-stimulated FPE, whereas the role of PI 3′-kinase appears to be minimal and/or cell-type dependent.

EXPERIMENTAL PROCEDURES

Cells. Cell lines were maintained at 37°C in a 5% CO_2-95% air atmosphere. Media and additives were purchased from Life Technologies (Grand Island, NY) unless otherwise noted. All media contained 2 mM glutamine (JRH Biosciences, Lenexa, KS), 100 U/ml penicillin (JRH Biosciences), and 100 μg/ml streptomycin (JRH Biosciences).

Rat-1, HIRc-B, and A/K1018-B cells (28, 30–32, 51) were generous gifts from Drs. D. A. McClain and J. M. Olefsky (University of California, San Diego, CA) and from A. Ullrich (Genentech, South San Francisco, CA). Rat-1 fibroblasts were maintained in minimal essential medium (with Earle's salts) supplemented with 10% (vol/vol) fetal calf serum (FCS). The mutant cell lines were grown in F-12/Dulbecco's modified Eagle's medium (1:1) deficient in hypoxanthine and thymidine and supplemented with 10% (vol/vol) FCS. NIH 3T3 HIR 3.5 cells and C127 HIR 4–60 cells were generously provided by Dr. J. Whittaker (State University of New York, Stonybrook, NY) and were grown in DMEM supplemented with 10% (vol/vol) FCS. Chinese hamster ovary (CHO)-T cells were a gift from Dr. R. A. Roth (Stanford University, Palo Alto, CA) and were grown in Ham's F-12 medium supplemented with 10% (vol/vol) FCS. H35 cells were a gift from Dr. J. W. Koontz (University of Tennessee, Knoxville, TN) and were maintained in low glucose-DMEM supplemented with 5% (vol/vol) FCS and 5% (vol/vol) calf serum. 32D cells and WEHI cells that were used to prepare conditioned medium, a source of interleukin-3 necessary for the growth of 32D cells, were described previously (54). Brown adipose tissue (BAT) cells were a gift from Drs. U. C. Kozak and L. P. Kozak (Jackson Laboratory, Bar Harbor, ME) and were grown in DMEM supplemented with 10% (vol/vol) FCS, biotin (0.33 μM final concentration), calcium pantothenate (0.17 μM final concentration), and ascorbic acid (1.0 mM final concentration; Sigma, St. Louis, MO). Because BAT cells are trypsin sensitive, collagenase or mechanical methods were employed to release the cells from flask surfaces.

Addition of agents. Regular insulin (Pork; Novo Nordisk, Princeton, NJ) was stored at 4°C and diluted in DMEM-1% BSA. 5-(*N*, *N*-dimethyl)-amiloride and amiloride (Sigma Chemical) were dissolved in Me_2SO at 60 μM and were diluted 20-fold in media for final concentrations of 3 mM amiloride and 5% (vol/vol) Me_2SO. Wortmannin (Sigma) was dissolved in Me_2SO to give a 10 mM stock solution and was stored at −20°C until use. Final concentrations of wortmannin in media contained 0.1% (vol/vol) Me_2SO. The mitogen-activated protein kinase kinase (MEK) inhibitor PD-98059 (1, 10), a generous gift from Dr. Alan Saltiel (Parke-Davis Warner-Lambert, Ann Arbor, MI), was dissolved in Me_2SO (20 mM) and stored at −20°C until use. Final concentrations of PD-98059 were 100 μM in 0.5% (vol/vol) Me_2SO; controls were treated in parallel with an equivalent concentration of Me_2SO.

Measurement of FPE in adherent cell lines. Two days before each experiment, cells were plated in normal growth medium at a concentration of 3×10^5 cells/well in 24-well plates (Costar, Cambridge, MA) and incubated overnight at 37°C. Eighteen to 24 h later, the cells were washed in phosphate-buffered saline (PBS) and incubated overnight (16–20 h) at 37°C in serum-free DMEM-1% BSA to make them quiescent. Cells were treated with 70 nM insulin in all experiments except where indicated. The fluid phase marker fluorescein isothiocyanate (FITC)-conjugated dextran (FD; molecular weight = 70,000; Molecular Probes, Eugene, OR) was dissolved in starvation medium and added to each well to a final concentration of 1 mg/ml. After various times of exposure to FD, the dye solution was aspirated, and each well was immediately washed with ice-cold PBS containing 1 mg/ml BSA (US Biochemical, Cleveland, OH), followed by two washes with ice-cold PBS. After the last PBS wash, 0.200 ml of 0.05% (wt/vol) trypsin (JRH Biosciences) in PBS was added. The plates were incubated on ice for ~10 min, until the cells were released from the plastic. Next, 0.165 ml of PBS containing 10% (vol/vol) FCS was added to each well to inactivate the trypsin, and the cells were transferred to Falcon tubes (Falcon 2052; Becton-Dickinson, Lincoln Park, NJ). Formaldehyde (0.135 ml of 3.7%) in PBS containing 10% FCS was added to each tube and mixed gently; the final formaldehyde concentration was 1%. The cells were stored at 4°C until analysis. Fluorescence in individual cells was measured using fluorescence-activated cell sorters (FACS) within 2 days of each experiment. The FACStar Plus and FACScan Flow Cytometers (Becton-Dickinson, Mountain View, CA) were equipped with argon lasers operating at 488 nm and 50 mW. FITC fluorescence was determined using a 530- or 30-nm filter. Fluorescence intensity was recorded only from cells that were alive during the FD incubation; these cells exhibited characteristic size and scatter factors, gating parameters that were determined before analysis. Data were analyzed by the Consort 32 utilizing the LysysII analysis and

software package. In each sample, the fluorescence of ~5,000 cells was measured, and these data were used to calculate the mean fluorescence per cell. At least three samples were analyzed for each treatment condition. Data points represent means ± SD of the replicate sample population means.

HRP (Sigma type II) was also used as a marker of FPE (39). Typically, cells were incubated with HRP (final concentration of 2 mg/ml in DMEM) and then washed as described above, trypsinized, and resuspended in 10% FCS to inhibit the trypsin. Cells were then pelleted, washed in PBS, and frozen at −20°C until analysis. HRP activity was measured spectrophotometrically as described (48). The initial rate of increase in absorbance at 460 nm, which was linear for 1–2 min, was used to calculate the concentration of HRP in each sample by comparison with rates observed with standard HRP solutions.

Measurement of FPE in 32D cells. Before each experiment, cells were made quiescent by incubation at 37°C for at least 2 h in DMEM-1% BSA. For each sample, 3×10^5 quiescent cells were treated with the indicated agents and 1 mg/ml FD (final concentration). After incubation with FD at 37°C, the cells were chilled on ice and centrifuged for 2 min at 3,000 *g* at 4°C. The dye solution was aspirated, and each cell pellet was immediately washed with ice-cold PBS containing 1 mg/ml BSA, followed by two washes with ice-cold PBS. After the last PBS wash, the cells were fixed in 250 µl of 1.0% formaldehyde (wt/vol) in PBS, transferred to Falcon tubes, and stored at 4°C until FACS analysis as detailed above.

Measurement of endosome recycling. Endosomes in quiescent HIRc-B cells were loaded with FD by incubating the cells for 2 h at 37°C in DMEM containing 1 mg/ml FD. Cells were then washed one time in ice-cold PBS containing 1 mg/ml BSA and two times in PBS. DMEM-1% BSA was then added to the cells (0.3 ml/well), followed by a further incubation at 37°C for the indicated times. Cells were washed in ice-cold PBS, trypsinized, and fixed. FD fluorescence remaining in the cells was quantitated by FACS analysis as described above.

Northern blot analysis of insulin receptor mRNA in 32D cell lines. Total RNA was prepared from log phase 32D cell cultures using the TriReagent-RNA/DNA/Protein Isolation Reagent according to the manufacturer's protocol (Molecular Research Center, Cincinnati, OH). RNA (20 µg) was fractionated on 2.2 M formaldehyde-1.2% agarose gels, transferred to Nytran membrane (Schleicher and Schuell, Keene, NH), and hybridized with a 1.1-kb *Eco*R I fragment of pSG5-HIRc (11) encoding part of the α-subunit of the human insulin receptor cDNA. The probe was labeled using the Random Primers DNA labeling system according to the manufacturer's protocol except that labeling was done for 4 h (Life Technologies).

Western blots of the insulin receptor and IRS-1 in 32D cell lines. Equal numbers of cells were concentrated by centrifugation from exponentially growing cultures of 32D, 32D/IR, 32D/IRS-1, and 32D/IR/IRS-1 cells (54). The pellets were washed two times in ice-cold PBS and resuspended in sample buffer containing 40% glycerol, 1.4 M β-mercaptoethanol, 4% SDS, 0.025 M Tris, and 0.1% bromphenol blue. Samples (~100 µg protein) were subjected to electrophoresis on 9% SDS-polyacrylamide gels and transferred to nylon membranes [polyvinylidene difluoride (PVDF), 0.2 µm; Bio-Rad, Hercules, CA]. After blocking the membranes in Tris-buffered saline (TBS; 10 mM Tris, pH 7.5, and 100 mM NaCl) containing 5% (wt/vol) nonfat dry milk and 0.05% (vol/vol) Tween 20, the membranes were incubated for 1 h in the same blocking solution with a rabbit antibody to IRS-1 (catalog no. 06–248; Upstate Biotechnolongy, Lake Placid, NY) used at a dilution of 1:1,000. Blots were washed four times (at least 10 min each wash) in TBS-Tween and then incubated for 1 h with HRP-conjugated goat anti-rabbit antibody diluted 1:5,000 in the blocking solution. Again, four washes in TBS-Tween were performed as before, and the bands were visualized using the enhanced chemiluminescence reagents (Amersham, Arlington Heights, IL). Blots were then stripped, reblocked, and reprobed with a rabbit antibody to the insulin receptor (catalog no. sc-710; Santa Cruz Biotechnology, Santa Cruz, CA) used at a dilution of 1:1,000 in blocking buffer. Subsequent steps were performed as described above.

Isolation of BAT cell lines expressing Ras and dominant negative 17N Ras. Vectors pZIPNeoSV(X) and pZIP-RasH(17N) for expression of the dominant negative 17N mutant of H-Ras were kindly provided by Dr. Channing Der (University of North Carolina, Chapel Hill, NC; see Refs. 8 and 40). BAT cells of line B4–4 were plated at 1×10^6 cells/100 mm dish (Costar) 2 days before transfection. Approximately 20 µg of plasmid DNA were transfected in cells using the BES-calcium phosphate-DNA precipitation protocol as described (17). Because the wild-type H-Ras expression vector, pHO6T1, used in these experiments did not contain an intrinsic selectable marker, the plasmid pSV2Neo was cotransfected with it at a ratio of 1:10 (pSV2Neo-pHO6T1; see Ref. 8). Cells were selected for neomycin resistance initially in medium supplemented with 250 mg/l Geneticin (Life Technologies). After 2 wk, survivors were replated at $\sim 1 \times 10^6$ cells/100-mm dish in medium containing 500 mg/l Geneticin. Resistant colonies were picked using a pipet tip (BAT cells are trypsin sensitive) and were placed in 24-well plates (Costar), where they were allowed to grow to confluence before expanding to 100-mm dishes. Colonies that overexpressed Ras or the 17N dominant negative mutant were identified by Western blot analysis of whole cell lysates (100 µg/lane) that had been separated on 12% SDS-PAGE gels and transferred to nylon membranes (PVDF, 0.2 µm; Bio-Rad) as described (8). After blocking membranes in TBS (10 mM Tris pH 7.5, 150 mM NaCl) containing 5% nonfat dry milk and 0.05% Tween 20 for 1 h at room temperature, the membranes were incubated overnight at 4°C in the same blocking solution containing a rat monoclonal antibody to Ras [v-H-Ras (259): sc-35; Santa Cruz Biotechnology] used at a dilution of 1:300 (vol/vol). After four washes of at least 10 min each in TBS-Tween, membranes were incubated for 1 h in blocking solution containing an HRP-conjugated rabbit anti-rat antibody at a dilution of 1:3,000. After washing as before, bands were visualized using chemiluminescence reagents. Clones that overexpressed the Ras proteins were expanded for further analysis of insulin-stimulated FPE.

Western blotting for MEK. Cells plated in 24-well plates as described above were made quiescent by culturing in DMEM-1% BSA overnight; the cells were pretreated with the MEK inhibitor PD-98059 (1, 10) in 0.5% Me_2SO or with 0.5% Me_2SO alone for 30 min at 37°C and then were treated with 70 nM insulin (final concentration) for 5, 10, 15, 20, or 25 min in DMEM-1% BSA or with DMEM-1% BSA as a control. At the end of the treatment, the medium was aspirated from the wells, and SDS-PAGE sample buffer was added directly to the cells. Samples were collected in Eppendorf tubes, sonicated to reduce viscosity, and loaded on 12% SDS-PAGE gels. After electrophoresis and transfer to PVDF membranes, blots were blocked in a solution of 4% BSA-TBS-Tween (10 mM Tris, 100 mM NaCl, and 0.05% Tween) and incubated for 1 h at room temperature with rabbit anti-active (phospho) MEK antibody (Promega, Madison, WI) used at a dilution of 1:20,000 in the same blocking buffer. Blots were washed extensively (at least 4 times for 15 min each) in TBS-Tween and then with the secondary antibody (HRP-conjugated goat anti-rabbit) at a dilution of 1:5,000 in the BSA blocking buffer for 1 h at room

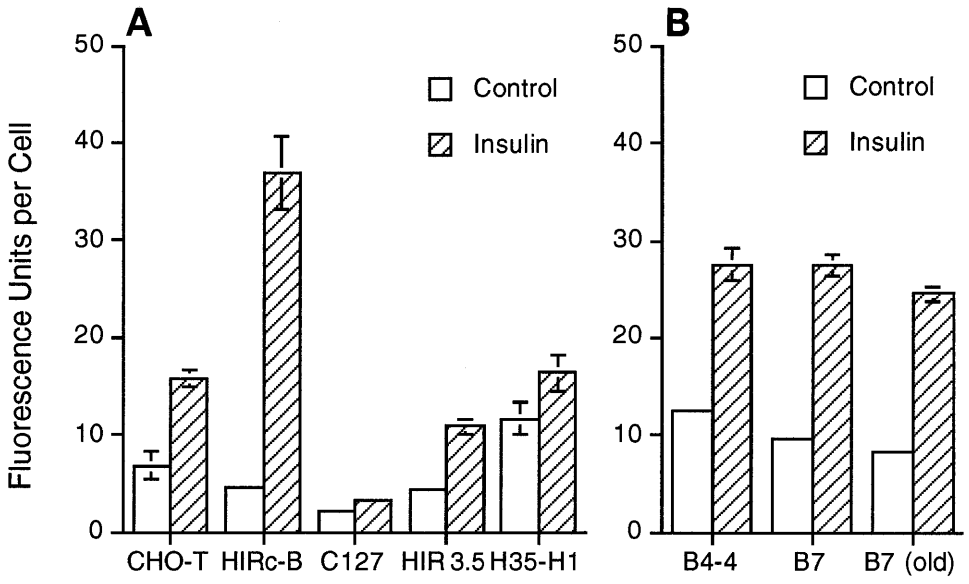

Fig. 1. Effect of insulin on fluorescein isothiocyanate-conjugated dextran (FD) accumulation in insulin-sensitive cell lines. *A*: quiescent cells were treated with 70 nM (hatched bars) insulin or a control solution (DMEM-1% BSA; open bars) for 90 min at 37°C. FD was added for the last 30 min. *B*: adipose tissue cell lines were tested for insulin-stimulated fluid phase endocytosis (FPE) essentially as described in *A*, except that cells were incubated with FD ± insulin for 30 min at 37°C. Cells were then washed and fixed for fluorescence-activated cell sorter (FACS) analysis. Bars represent mean ± SD fluorescence per cell from 5 samples in *A* and 3 samples in *B* (5,000 cells analyzed/sample). Differences between insulin-stimulated and control samples were highly significant ($P < 0.0005$) for each cell line, using Student's *t*-test. CHO, Chinese hamster ovary.

temperature. Blots were washed as before, and bands were visualized using the Amersham chemiluminescence reagents as described above.

RESULTS

Initial experiments were done to determine which insulin-responsive cell lines exhibited the highest rate of insulin-stimulated FPE. The intracellular accumulation of the fluorescent fluid phase marker FD was measured under control and insulin-stimulated conditions (70 nM insulin) in an immortalized liver cell line (H35), BAT-derived cell lines [BAT B4–4, B7, and B7(old)], and several cell lines overexpressing the human insulin receptor, including CHO-T cells, Rat-1 fibroblasts (HIRc-B), C127 cells (C127 HIR 4–60), and NIH 3T3 fibroblasts (NIH 3T3 HIR 3.5; Fig. 1, *A* and *B*). In the presence of insulin, the relative intracellular fluorescence was increased 0.5- to 8-fold over that measured in the unstimulated cell lines.

HIRc-B cells, which express ~1.2 × 10^6 insulin receptors/cell (30), were used for further experiments, since they exhibited the strongest response to insulin with regard to accumulation of FD (Fig. 1). The use of FD as a marker of FPE in these cells was validated by showing that its uptake was nonsaturable with increasing FD concentration or time of incubation (Fig. 2, *A* and *B*). In addition, another commonly used marker of FPE, HRP, was also internalized by HIRc-B cells more rapidly in the presence of insulin (4-fold increase over basal, data not shown).

Fluorescence microscopy of the insulin-stimulated HIRc-B cells after incubation with FD revealed the presence of large fluorescent vesicles (0.6–4.4 μm diameter) resembling macropinocytic vesicles (43). Smaller

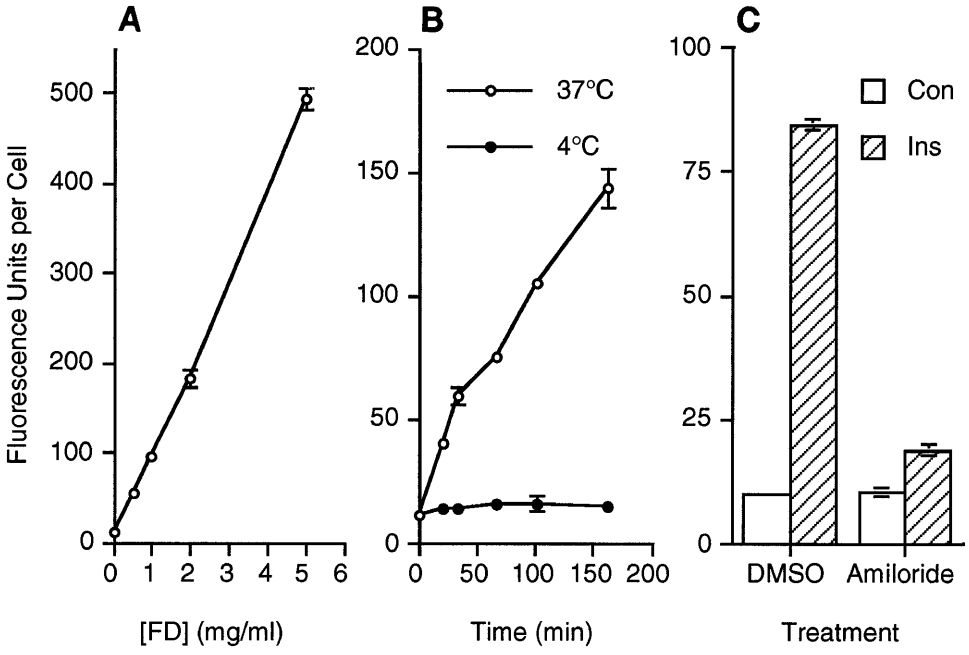

Fig. 2. Characteristics of FD uptake by HIRc-B cells: dependence on FD concentration, time, temperature, and sensitivity to amiloride. *A*: quiescent cells were incubated with the indicated concentration of FD ([FD]) for 90 min at 37°C. *B*: quiescent cells were incubated with 1 mg/ml FD either at 37°C (○) or 4°C (●) for the indicated lengths of time. *C*: quiescent cells were pretreated with amiloride (3 mM in 3% Me_2SO) or a control solution (3% Me_2SO) for 10 min before addition of FD [control (Con); 1 mg/ml, final concentration; open bars] or FD and insulin (Ins; 70 nM, final concentration; hatched bars). Cells were incubated for 30 min at 37°C and then were washed and fixed, and intracellular fluorescence was analyzed by FACS. Data points and bars represent means ± SD of triplicate samples. DMSO, Me_2SO.

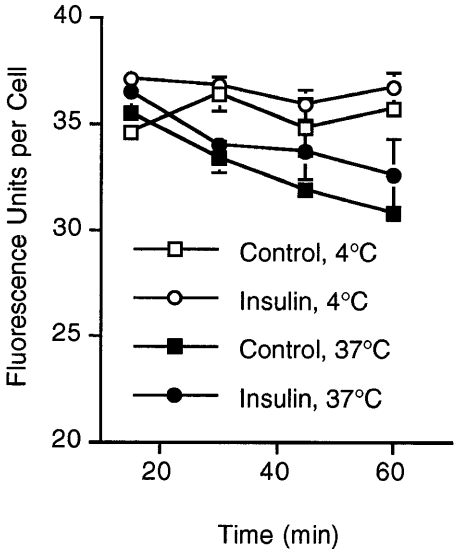

Fig. 3. Effect of insulin on recycling of FD-loaded endosomes to the plasma membrane. Quiescent, FD-loaded HIRc-B cells were incubated for various lengths of time at 37°C or 4°C in DMEM-1% BSA (squares) or in DMEM-1% BSA and 70 nM insulin (circles). At the indicated times, cells were washed and fixed, and the fluorescence remaining in the cells was quantified by FACS analysis. Each point represents the mean ± SD fluorescence values from triplicate samples.

vesicles were also apparent, suggesting that some uptake might be occurring in vesicles derived from clathrin-coated pits, which are generally 100–150 nm in diameter (data not shown). To determine the proportion of FD uptake in HIRc-B cells that was independent of receptor-mediated endocytosis, we took advantage of the fact that FPE is more sensitive to amiloride than receptor-mediated endocytosis (55). HIRc-B cells pretreated with 3 mM amiloride exhibited only 12% of the insulin-stimulated FPE observed in control cells (Fig. 2*C*), suggesting that most of the insulin-stimulated FD internalization in this system was amiloride sensitive and thus due to FPE.

The results shown in Fig. 2*B* suggested that insulin-stimulated FD uptake was most rapid in the initial 30 min of treatment and then continued at a somewhat slower rate. This apparent decrease in uptake rate has been attributed to the return of vesicles containing the marker to the plasma membrane, followed by release of the marker in the extracellular fluid. To assess the effect of insulin on this recycling of endocytic vesicles, we preloaded HIRc-B cells with FD and then, after careful washing, incubated them in marker-free medium at 37°C or 4°C in the presence or absence of insulin. At the indicated times, cells were harvested and the relative amount of intracellular FD was measured. There was a measureable level of endosome recycling to the plasma membrane under basal conditions (Fig. 3). However, the level of FD remaining in the insulin-treated cells was similar to or greater than that seen in the control cells, indicating that insulin did not increase the recycling of marker-filled endosomes in HIRc-B cells under these conditions.

We also examined the dose dependence of insulin-stimulated FPE in the HIRc-B cells. The stimulatory effect of insulin on FPE was concentration dependent, with half-maximal stimulation occurring between 0.07 and 0.7 nM insulin (Fig. 4*A*). To assess the time course of the insulin effect, HIRc-B cells were treated with 70 nM insulin for the indicated times and exposed to FD for the final 15 min (Fig. 4*B*). After 15 min of insulin treatment, the rate of FD uptake was essentially maximal, at 3.7 times control. This rate remained elevated for at least 4 h, at which time it was 3.8 times control (Fig. 4*B*).

Insulin-stimulated FPE is dependent on insulin receptor tyrosine kinase activity. The HIRc-B cell line is a derivative of Rat-1 cells, a fibroblast line that expresses only ~1,700 endogenous insulin receptors/cell (30). To determine whether the insulin receptor and its intrinsic protein tyrosine kinase activity were necessary for mediating insulin-stimulated FPE, the response of

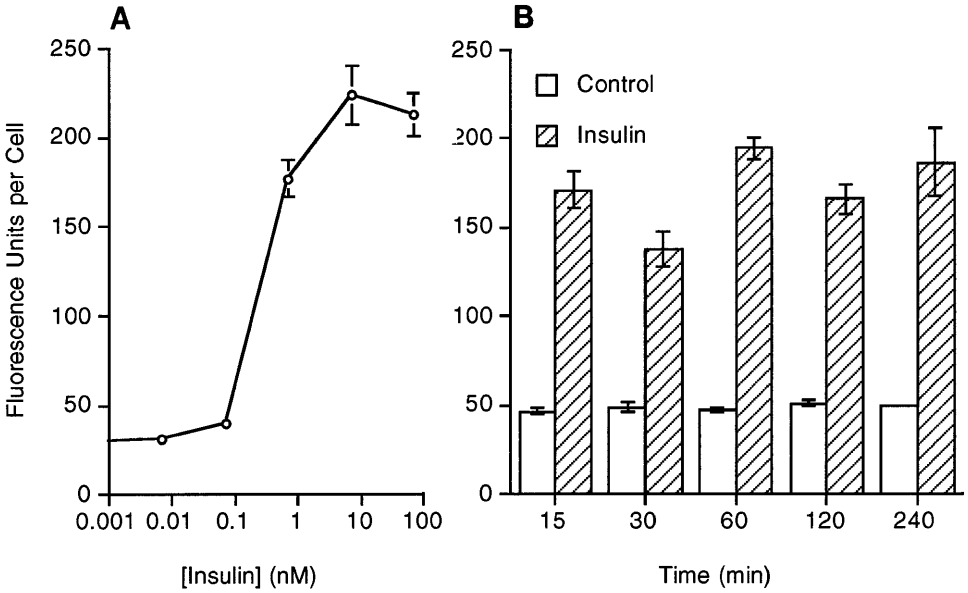

Fig. 4. FD accumulation in HIRc-B cells: dose response to insulin and time course. *A*: quiescent HIRc-B cells were treated with the indicated concentrations of insulin ([Insulin]) in the presence of FD for 60 min. Intracellular fluorescence was then quantified by FACS analysis. *B*: quiescent HIRc-B cells were treated with 70 nM insulin (hatched bars) or carrier alone (open bars) for the indicated lengths of time. FD was included for the last 15 min of each treatment. Relative fluorescence per cell was then assessed by FACS analysis. Bars represent the mean ± SD average relative fluorescence per cell from 6 samples. Difference between insulin and control was highly significant ($P < 0.0005$) at each time point, using Student's *t*-test.

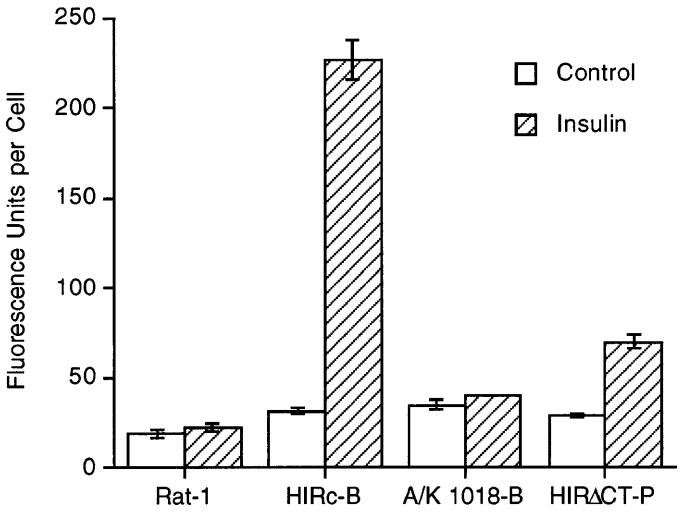

Fig. 5. Effect of insulin on FD accumulation in cells expressing normal or mutant insulin receptors. Quiescent cells were treated with either 70 nM insulin and FD (hatched bars) or FD alone (open bars) for 60 min, followed by FACS analysis. Each bar represents the mean ± SD fluorescence per cell from 6 samples. Difference between insulin and control was significant for HIRc-B ($P < 0.0005$), A/K1018-B ($P < 0.002$), and HIRΔCT ($P < 0.0005$). Difference between the insulin and control treatments was not significant for Rat-1 fibroblasts.

Rat-1 cells to insulin was compared with that of HIRc-B cells. As shown in Fig. 5, the relative fluorescence measured in the parental Rat-1 cells treated with insulin (70 nM) was only 1.1-fold greater than that measured in the unstimulated cells. HIRc-B cells treated in parallel exhibited a 7.2-fold increase in response to insulin stimulation, indicating that the overexpressed insulin receptors were mediating this response.

The requirement for the tyrosine kinase activity of the insulin receptor was determined by investigating the response of a Rat-1 cell line that expresses a mutant form of the human insulin receptor, Rat-1 A/K1018-B cells. This line expresses $\sim 2.2 \times 10^5$ receptors/cell (30). These receptors have a single lysine-to-alanine substitution at the ATP-binding site that completely abrogates intrinsic tyrosine kinase activity but does not significantly affect insulin binding (29, 30). As shown in Fig. 5, FPE was only slightly stimulated by insulin treatment of cells expressing the A/K1018 receptor; the observed 1.1-fold stimulation was similar to that observed in the parental Rat-1 cells and could be due to the presence of small numbers of wild-type endogenous rat insulin receptors in these cells.

We also examined insulin-stimulated FPE in HIRΔCT-P cells, another derivative of the Rat-1 cell line (28, 31). HIRΔCT-P cells express 2.5×10^5 truncated human insulin receptors per cell. The ΔCT mutant receptor lacks the carboxy-terminal 43 amino acids of the β-subunit. It has been observed that autophosphorylation of two tyrosines within this region increases the tyrosine kinase activity of the insulin receptor and that the Rat-1 cells expressing this receptor show blunted insulin-stimulated 2-deoxy-D-glucose uptake and activation of glycogen synthase compared with cells expressing the wild-type receptor (28). Not unexpectedly, the response of these cells to insulin was less than that observed in the HIRc-B cells (2.4-fold increase in FPE compared with 7.2-fold) but was still consistently greater than that seen in the parental Rat-1 cells (Fig. 5).

IRS-1 is involved in signaling insulin-stimulated FPE. Insulin-stimulated mitogenesis is mediated though the 180-kDa intracellular protein, IRS-1, that is phosphorylated by the activated insulin receptor (reviewed in Ref. 36). We evaluated the role of IRS-1 in insulin-stimulated FPE using the 32D cell line, a hematopoietic precursor line that lacks endogenous IRS-1 and expresses low numbers of insulin receptors (~500/cell). In the parental 32D cell line, the basal level of FPE was almost undetectable. Insulin treatment of these cells increased FPE so that the rate was similar to the basal rate of FPE observed in the lines expressing either or both exogenous insulin receptor (32D/IR) and IRS-1 (32D/IRS-1, 32D/IR/IRS-1; Fig. 6*A*). 32D/IR cells responded to insulin with a reproducible decrease in FPE. In contrast, the rate of FPE increased five- to sixfold over basal in response to insulin in 32D/IRS-1 cells and in 32D/IR/IRS-1 cells. These two cell lines expressed approximately equal amounts of the IRS-1 protein, as demonstrated by Western blotting (Fig. 6*B*). We verified that FD behaved as a true fluid phase marker in these cells using the 32D/IR/IRS-1 line and found that FD uptake was linear with incubation time, FD concentration, and temperature (Fig. 7, *A-C*). Furthermore, in cells that were pretreated with 3 mM amiloride, insulin-stimulated FD uptake was negligible; thus, as in the other insulin-responsive cell types, FD internalization appeared to be mediated though FPE (Fig. 7*D*).

Because we had anticipated that 32D/IRS-1 cells, which express few insulin receptors, would show little insulin-stimulated FPE, we verified the identity of all four cell lines by their antibiotic resistance, by Northern blotting using a probe for the human insulin receptor mRNA (the mRNA was only observed in the 32D/IR and 32D/IR/IRS-1 lines, as expected; data not shown), and by Western blotting for the insulin receptor and IRS-1 (Fig. 6*B*). We also measured basal and insulin-stimulated FPE in another 32D/IRS-1 clone (661.5) with essentially the same results as the clone shown in Fig. 6 (clone Ic). Thus the low numbers of endogenous insulin receptors present in the 32D/IRS-1 cells (~500/cell) were apparently sufficient to mediate insulin-stimulated FPE in the presence of IRS-1. We conclude that the presence of IRS-1 was responsible and necessary for the increased rate of insulin-stimulated FPE observed in 32D/IRS-1 and 32D/IR/IRS-1 cells compared with 32D or 32D/IR cells.

Overexpression of wild-type H-Ras augments insulin-stimulated FPE, whereas expression of a dominant negative 17N Ras represses it. A BAT cell line (BAT B4–4) was stably transfected with wild-type H-Ras or the dominant negative 17N H-Ras constructs (40). Clones that expressed the exogenous proteins were selected by Western blot analysis of whole cell lysates,

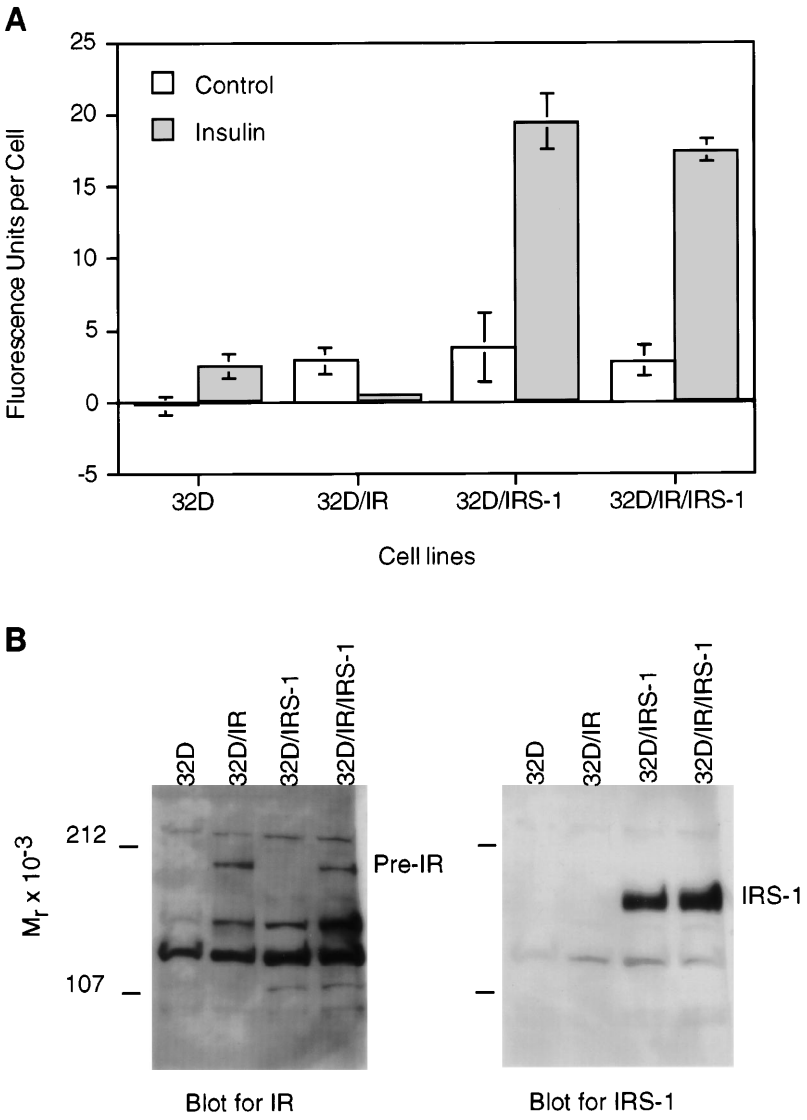

Fig. 6. Effect of insulin receptor (IR) and insulin receptor substrate-1 (IRS-1) expression on insulin-stimulated uptake of FD in 32D cells. *A*: quiescent 32D cell lines were incubated with insulin and FD (filled bars) or FD alone (open bars) for 30 min at 37°C or 4°C. Bars indicate the mean ± SD fluorescence of at least 3 samples, corrected for FD fluorescence measured at 4°C, for each experimental condition. Note that basal fluorescence of 32D/IRS-1 cells incubated with FD at 4°C was often 2- to 3-fold higher than that of identically treated 32D cells. *B*: proteins from each 32D cell line were separated, blotted, and probed with antibodies to IRS-1 and IR, as described in EXPERIMENTAL PROCEDURES. IR antibody cross-reacted with a protein migrating near the expected size of the IR α-subunit [relative molecular weight (M_r) = 135,000]. However, this protein was present at similar levels in all 4 cell lines and is apparently not related to the receptor. Precursor of the IR runs at M_r = ~200,000 and was detected only in the 32D/IR and 32D/IR/IRS-1 cells as expected.

as shown in Fig. 8*A*. The Ras protein was identified by its size on SDS-PAGE gels (~21 kDa) and its reactivity with both a nonspecific Ras antibody (Fig. 8*A*) and a second antibody that selectively detected the H-Ras expressed from the transfected plasmid (not shown). Good expression was observed in several clones of the wild-type H-Ras (shown are clones 2–2 and 5) and in one clone of the dominant negative 17N Ras mutant.

FPE in response to insulin was measured in these cell lines. The dose-response curve shown in Fig. 8*B* indicated that expression of wild-type Ras augmented the response to insulin at every concentration used. Both clones expressing the wild-type Ras protein showed greater insulin-stimulated FPE than the untransfected cells. The insulin-stimulated FPE in these Ras clones was also greater than that in BAT B4–4 cells transfected with the vector alone that were used as controls in other experiments (not shown). Conversely, the expression of the dominant negative 17N Ras inhibited insulin-stimulated FPE at every concentration where stimulation of FPE was observed in the control cells (Fig. 8*B*). The basal level of FPE was largely unaffected by the expression of the dominant negative Ras (9.7 ± 2.7 relative fluorescence units/cell for the controls compared with 13.6 ± 1.0 for the mutant, means ± SD). These results suggest that Ras participates in the signaling pathways between the activated insulin receptor and the cellular machinery for FPE.

Ras activates the MAP kinase cascade, an important pathway for transmitting mitogenic signals from growth factor receptors to the nucleus. Recently, PD-98059, a relatively specific inhibitor of the MEK protein, has been developed (10). This inhibitor appears to have no effect on a variety of other protein kinases in cells, including MAP kinase, src tyrosine kinase, and Raf-1 (1). To assess whether the activity of MEK and the MAP kinase pathway were essential for insulin stimulation of FD uptake in BAT cells, we pretreated one set of cells with 100 μM PD-98059 for 30 min before measuring FD uptake in the presence and absence of insulin. We found that insulin-stimulated FD uptake in the cells pretreated with the MEK inhibitor was only slightly less (by ~13%) than that seen in the controls (Fig. 9). To verify that PD-98059 was inhibiting MEK, we per-

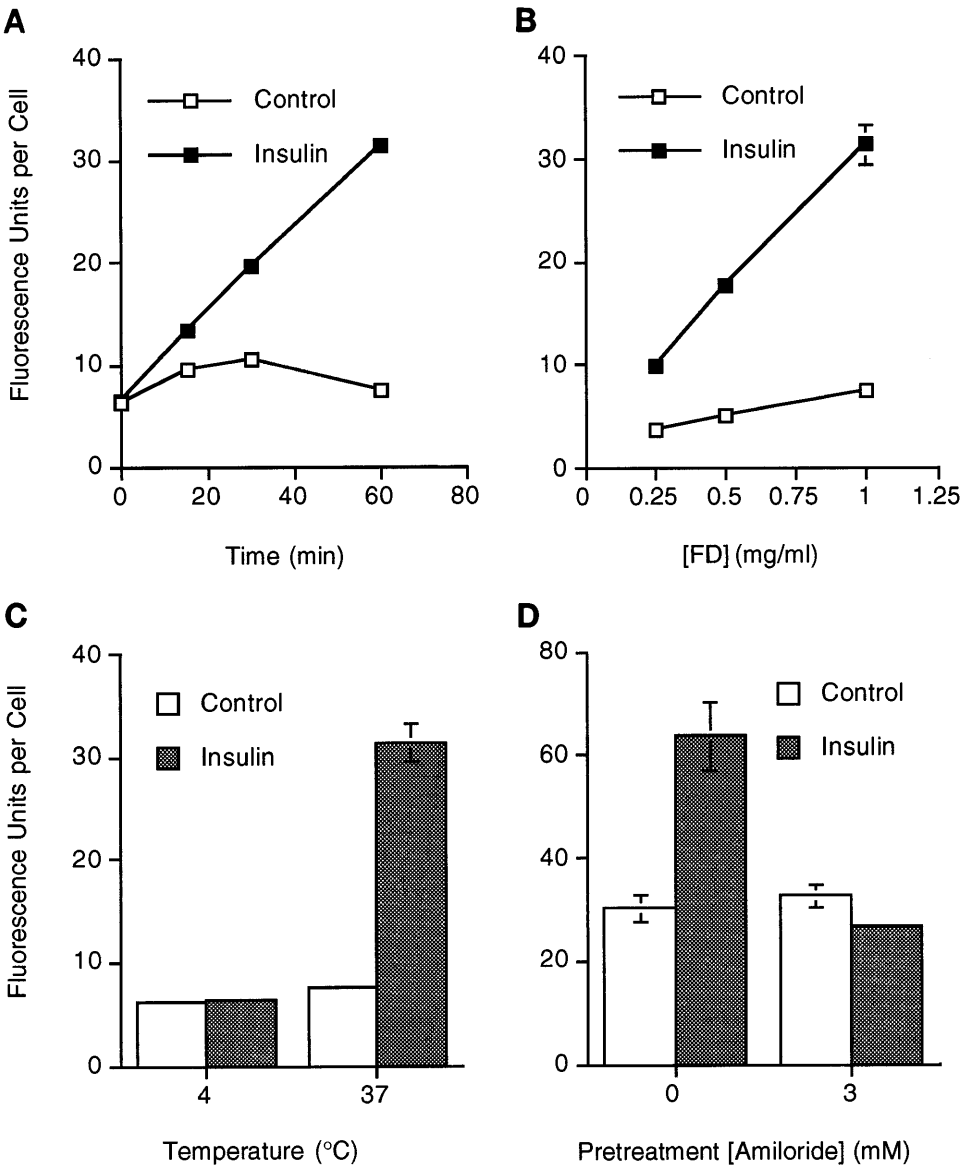

Fig. 7. Effect of time, FD concentration, temperature, and amiloride on insulin-stimulated accumulation of FD in 32D/IR/IRS-1 cells. *A*: quiescent cells were treated with insulin and FD (■) or FD alone (□) for the indicated times at 37°C and then were processed for FACS analysis as detailed in EXPERIMENTAL PROCEDURES. *B*: quiescent cells were incubated with the indicated concentrations FD (□) or FD and insulin (■) for 30 min at 37°C. *C*: quiescent cells were incubated for 60 min with FD and insulin (filled bars) or FD alone (open bars) at 4°C or 37°C. *D*: cells were pretreated with 3 mM amiloride or carrier alone (3% Me_2SO in DMEM-1% BSA) for 5 min at room temperature before addition of FD (open bars) or FD and insulin (filled bars). [Amiloride], amiloride concentration. Cells were incubated at 37°C for 30 min and then washed, fixed, and analyzed by FACS. In each experiment, data points and bars indicate means ± SD from triplicate samples at each condition.

formed a Western blot using an antibody specific for active (phosphorylated) MEK. A set of BAT cells was pretreated with either the inhibitor or with the 0.5% Me_2SO carrier alone and then with insulin. Two bands, one at 42 kDa and another less intense band at 44 kDa, consistent with the known relative molecular mass of the MEK proteins (9), were observed in the BAT cells 5, 10, and 15 min after stimulation with 70 nM insulin. No active MEK species were detected in the cells pretreated with the inhibitor, indicating that this pathway was effectively inhibited by PD-98059 under these experimental conditions (data not shown).

Effect of wortmannin, an inhibitor of PI 3′-kinase activity, on insulin-stimulated FPE in HIRc-B, BAT, and 32D cells. PI 3′-kinase activity is stimulated when the regulatory p85 subunit of the enzyme binds to phosphotyrosines in IRS-1 (36). The fungal metabolite wortmannin inhibits PI 3′-kinase activity in intact cells with half-maximal inhibition generally occurring between 5 and 10 nM (52). To assess whether PI 3′-kinase had a role in insulin-stimulated FPE, the HIRc-B, BAT, and 32D/IR/IRS-1 cells were pretreated for at least 15 min with 100 nM wortmannin, and then insulin-stimulated FD uptake was assayed (Fig. 10). HIRc-B cells treated with 100 nM wortmannin exhibited 30–70% of the insulin-stimulated FD uptake seen in the untreated controls (70% for the experiment shown). In BAT cells treated under similar conditions, wortmannin-treated cells exhibited 85–95% of the insulin-stimulated FD uptake seen in controls. At concentrations of wortmannin expected to be more specific for PI 3′-kinase (1, 5, and 10 nM), there was no significant decrease in insulin-stimulated FPE in either the HIRc-B or the BAT cells (data not shown). Increasing the preincubation time with wortmannin to 1 h at 37°C also did not increase the inhibition in these cells. Interestingly, preincubating these cells with both 3 mM amiloride and 100 nM wortmannin completely abolished insulin-stimulated uptake of FD. This suggests that the amiloride-resistant component of insulin-stimu-

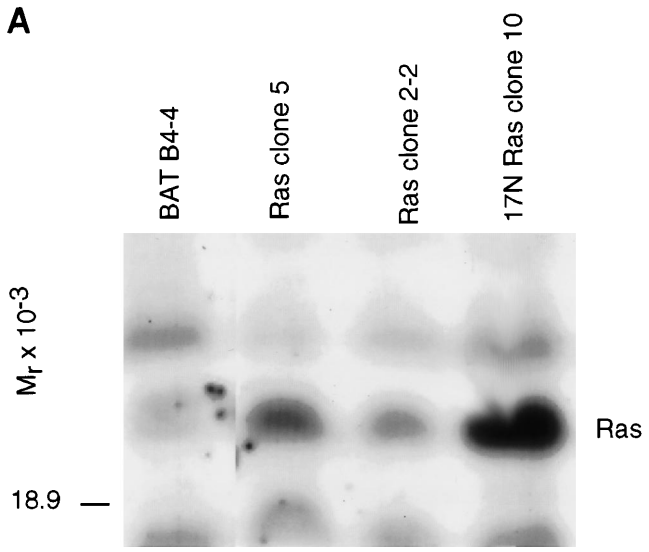

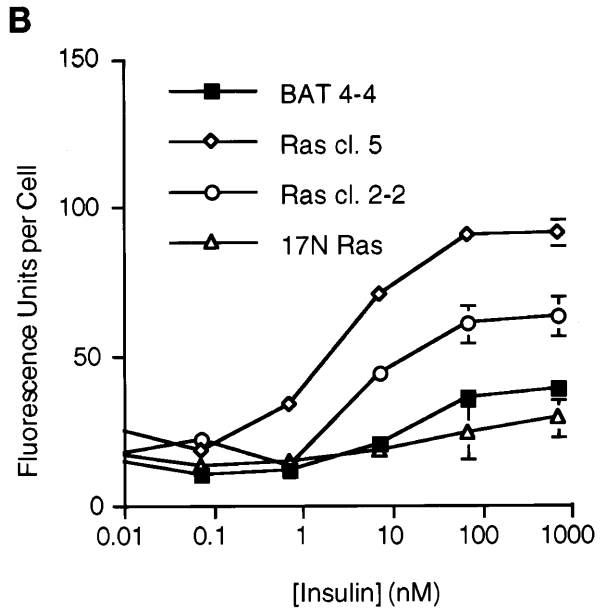

Fig. 8. Expression of exogenous Ras proteins and the effect on insulin-stimulated FPE in brown adipose tissue (BAT) cells. *A*: Ras expression was analyzed by Western blot using equal amounts of protein (~100 μg/lane) from untransfected BAT cell line B4–4 (*lane 1*) and clonal BAT cell lines expressing either the exogenous wild-type H-Ras (*lanes 2* and *3*) or the 17N dominant negative Ras mutant (*lane 4*). *B*: insulin-stimulated FPE was measured in quiescent BAT cell lines as detailed in EXPERIMENTAL PROCEDURES, except that cells were treated with increasing doses of insulin (0, 0.07, 0.7, 7, 70, and 700 nM) for 30 min at 37°C or 4°C. Points represent the mean fluorescence per cell ± SD of the triplicate samples, corrected for the fluorescence at 4°C. ■, Data from untransfected BAT cells; ◇, BAT/Ras clone (cl.) 5; ○, BAT/Ras clone 2–2; and △, BAT/17N Ras clone 10.

lated uptake (presumably mediated by clathrin-coated vesicles) is sensitive to wortmannin.

In contrast to the HIRc-B and BAT cells, treatment of the 32D/IR/IRS-1 cells with 100 nM wortmannin completely inhibited insulin-stimulated FPE (Fig. 10). Furthermore, insulin-stimulated FPE was inhibited at

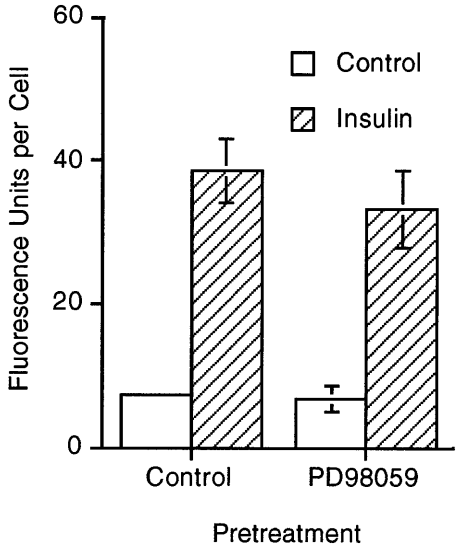

Fig. 9. Treatment of BAT cells with the mitogen-activated protein kinase kinase (MEK) inhibitor PD-98059: effect on insulin-stimulated FPE. BAT cells were treated with 100 μM PD-98059 in 0.5% Me_2SO or with 0.5% Me_2SO alone for 30 min at 37°C and then were treated with FD and insulin (hatched bars) or FD alone (open bars) for another 30 min at 37°C. Bars indicate the means ± SD of the replicates. Differences between insulin-stimulated levels of FPE in the 2 sets of samples were not significant ($P \leq 0.133$).

concentrations of wortmannin expected to be specific for PI 3′-kinase, with only 20% of insulin-stimulated FPE remaining in cells pretreated with 10 nM wortmannin (data not shown). These results suggest that PI 3′-kinase activity is required for insulin-stimulated FPE in the 32D/IR/IRS-1 cells.

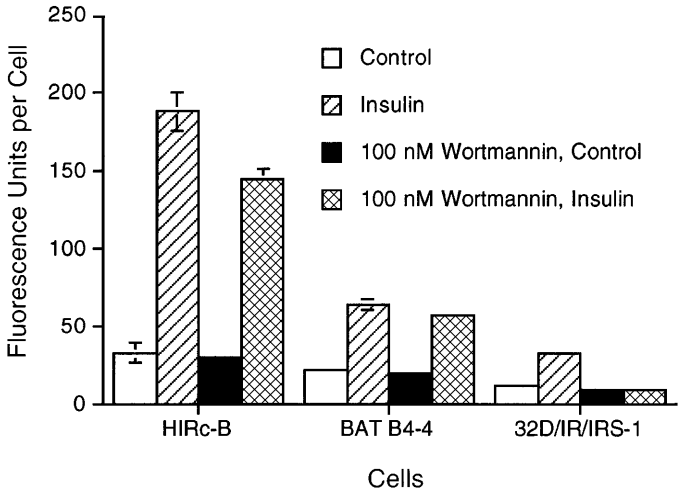

Fig. 10. Pretreatment of HIRc-B, BAT, and 32D/IRS-1 cell lines with 100 nM wortmannin: effect on insulin-stimulated FPE. Quiescent HIRc-B, BAT, and 32D/IR/IRS-1 cells were pretreated with 100 nM wortmannin in 0.01% Me_2SO (filled bars) or with 0.01% Me_2SO alone (open bars) for 15 min. Afterward, FD (filled bars) or FD and insulin (hatched and crosshatched bars) were added, and the cells were incubated for an additional 60 min at 37°C. Cells were pelleted, washed, fixed, and analyzed by FACS as indicated in EXPERIMENTAL PROCEDURES. Bars represent the mean ± SD fluorescence per cell from 3 replicates for BAT and 32D/IRS-1 cells and 6 replicates for HIRc-B cells.

DISCUSSION

Our findings in this study support the idea that increased FPE is a general response to insulin in cells that express its receptors (33). This response was observed in every insulin-sensitive cell line that we examined and has been observed by others in KB cells (24, 33), 3T3-L1 cells (14), rat H35 hepatoma cells (15), the human monocyte cell line U-937 (27, 38), *Xenopus* oocytes (34), and in primary cultures of rat adipocytes (13) and hepatocytes (35). However, one apparent exception is the insulinoma cell line bTC6-F7 in which insulin reportedly activates its receptor but does not increase FPE (60). The present study has identified the proximal components of the insulin-stimulated FPE pathway as the insulin receptor, its substrate IRS-1, and Ras. It is conceivable that one of these components is defective or absent in the bTC6-F7 cell line, uncoupling the activation of the receptor from FPE.

Our studies show that the tyrosine kinase activity of the insulin receptor is essential for insulin-stimulated FPE. Although the greatest increase in insulin-stimulated FPE was observed in HIRc-B cells, a Rat-1 cell line that overexpresses the normal human insulin receptor, no increase beyond that of the parental Rat-1 cell line was observed in the A/K1018-B line, which expresses a kinase-deficient mutant of the human insulin receptor. Previous work has shown that the receptor tyrosine kinase activity is required in these cells, not only for the mitogenic and metabolic effects of insulin (30) but also for the endocytosis of the insulin receptor and cell ruffling (4, 26, 30). The dependence of insulin-stimulated FPE on insulin receptor tyrosine kinase activity has not been examined previously, to our knowledge. Presumably, the tyrosine kinase activity would be essential to stimulation of FPE in all cell types that exhibit this response.

IRS proteins are phosphorylated by the activated insulin receptor and its relatives, the insulin-like growth factor receptors (36). IRS proteins are essential for insulin-stimulated mitogenesis (54) and appear to play a role in GLUT-4 glucose transporter recruitment to the plasma membrane (21, 41). Our studies showed that IRS-1 also plays a role in mediating insulin-stimulated FPE. The 32D cell line, which lacks IRS proteins, exhibited some insulin-stimulated FPE (Fig. 6). However, the level of insulin-stimulated FPE in 32D/IRS-1 cells was increased as much as sixfold over that of control 32D cells or 32D/IR cells. We also noted that cells expressing IRS-1 responded to insulin as strongly as those expressing both the insulin receptor and IRS-1. The small number of endogenous receptors (~500/cell; see Ref. 54) was thus sufficient for generation of the full response when IRS-1 was present. It is also noteworthy that the FPE response of cells to insulin is more sensitive than insulin induction of c-*fos* and *egr*-1. In HIRc-B cells, we showed that FPE was almost maximally stimulated at 0.7 nM insulin, whereas insulin-induced c-*fos* and *egr*-1 gene transcription was not observed until 10-fold more insulin was applied (50). This difference in response sensitivity is also likely to account for the fact that, in 32D cells, others have reported that overexpression of the insulin receptor was necessary to observe insulin-stimulated c-*fos* and *egr*-1 expression (16), whereas our present data indicate that endogenous receptors are sufficient for insulin-stimulated FPE in these cells (16).

The dependence of insulin-stimulated FPE on IRS proteins suggested that factors that bind to the IRS scaffold might be important mediators of insulin-stimulated FPE. Certain phosphotyrosines within the IRS-1 protein act as docking sites for GRB2/SOS, facilitating the interaction of the SOS guanine nucleotide exchange factor with Ras (47, 53). This association between SOS and Ras results in the conversion of inactive Ras-GDP to active Ras-GTP. Injection of Ras in quiescent fibroblasts has been shown to stimulate ruffling and FPE (5). The influence of exogenous wild-type Ras and the dominant negative 17N Ras on insulin-stimulated FPE was investigated in BAT cells. Stable overexpression of exogenous wild-type Ras proteins augmented insulin-stimulated FPE, whereas the mutant 17N Ras inhibited it (Fig. 8). These results strongly suggest that insulin-stimulated FPE is mediated through Ras (with the caveat that some contribution to this effect could potentially be due to the interaction of the overexpressed Ras proteins with components of other G protein-regulated processes that are involved in FPE, i.e., Rab5-regulated endocytic vesicle trafficking and Rac-regulated actin polymerization).

Ras itself has been shown to represent a point of bifurcation for signals emanating from activated receptor protein tyrosine kinases; signals to the nucleus are transmitted through the MAP kinase cascade, whereas signals to the membrane (for ruffling) are mediated by the Rac family of GTP-binding proteins (19, 20). Our experiments in the BAT cells using the specific MEK inhibitor PD-98059 indicate that the MAP kinase cascade is not involved in signaling insulin-stimulated FPE, at least under the conditions of these experiments (Fig. 9). Further experiments with dominant negative Rac proteins may show a role for Rac in insulin-stimulated FPE.

PI 3′-kinase has been implicated in vesicular trafficking due in part to its homology to the yeast protein, VSP34, a component of the lysosomal sorting apparatus. PI 3′-kinase activity is coprecipitated with most activated receptor protein tyrosine kinases (44) and may have a role in the internalization of activated receptors. PI 3′-kinase is also implicated in insulin-stimulated GLUT-4 translocation and growth factor-induced cell ruffling and FPE (reviewed in Ref. 22). Most of the evidence for PI 3′-kinase activity in ruffling and FPE has been obtained using wortmannin, an inhibitor of PI 3′-kinase activity (23, 24). We also used wortmannin to examine the role of PI 3′-kinase in insulin-stimulated FPE in HIRc-B, BAT, and 32D/IR/IRS-1 cells. However, the interpretation of our wortmannin inhibition experiments was complicated by two factors, namely, that higher concentrations of wortmannin have been shown to inhibit enzymes other than PI

3′-kinase, including myosin light chain kinase (37), and that a wortmannin-sensitive PI 3′-kinase activity has been shown to be required for the fusion of membrane folds in macropinocytic vesicles in macrophages (3). In our experiments, in 32D cells, insulin-stimulated FPE was sensitive to wortmannin at concentrations expected to be specific for PI-3 kinase (Fig. 10). However, the inference that PI 3′-kinase is involved in insulin-stimulated FPE in these cells is invalid if PI 3′-kinase activity is required for membrane fusion events, as it was in macrophages (both 32D cells and macrophages are of hematopoietic lineage).

In contrast to the results in 32D cells, wortmannin had no significant effect on insulin-stimulated FPE in either the BAT cells or the HIRc-B cells at nanomolar concentrations (Fig. 10). Our interpretation of these results was that a wortmannin-sensitive PI 3′-kinase activity was not essential for insulin-stimulated FPE in these cells. Recently, others have shown that wortmannin treatment also had minimal effects on either basal or insulin-stimulated FPE in 3T3-L1 fibroblasts, at concentrations at which it was inhibitory to trafficking of glucose transporters and transferrin receptors (18). However, wortmannin treatment has been shown to inhibit insulin-stimulated FPE and ruffling in CHO-T cells, underscoring the fact that the role of PI 3′-kinase may be cell-type specific (24, 60).

The physiological role of insulin-stimulated FPE has been the subject of considerable speculation (2, 25, 27, 57, 59) but remains unknown. An essential question that remains unanswered is the extent to which this process changes in parallel with the other biochemical pathways that are markedly altered in insulin-resistant states, such as type 2 diabetes and obesity. If, for example, patients developed severe insulin resistance in terms of glucose transport but remained normally sensitive to insulin in terms of FPE, one could imagine that the increased flux of extracellular nutrients in the cells might have deleterious consequences. An example might be the common clinical observation that type 2 diabetic patients typically gain weight when placed on the high doses of insulin often required to achieve normoglycemia in this insulin-resistant state. Studies of FPE in such insulin-resistant cells will be necessary to answer these and other intriguing questions about the physiological role of insulin-stimulated FPE and its possible alterations in pathological states.

We are very grateful to J. Michael Cook and Alan Fisher from the Duke Comprehensive Cancer Center Flow Cytometry Facility for performing the FACS analyses.

P. J. Blackshear was an Investigator and D. M. Pitterle was an Associate of the Howard Hughes Medical Institute during the course of these studies. M. F. White is currently an Investigator of the Howard Hughes Medical Institute.

Address for reprint requests: P. J. Blackshear, A2–05, National Institute of Environmental Health Sciences, Research Triangle Park, NC 27709.

Received 23 February 1998; accepted in final form 4 September 1998.

REFERENCES

1. **Alessi, D. R., A. Cuenda, P. Cohen, D. T. Dudley, and A. R. Saltiel.** PD 098059 is a specific inhibitor of the activation of mitogen-activated protein kinase kinase in vitro and in vivo. *J. Biol. Chem*. 270: 27489–27494, 1995.
2. **Al-Habori, M.** Mechanism of insulin action, role of ions and the cytoskeleton. *Int. J. Biochem*. 25: 1087–1099, 1993.
3. **Araki, N., M. T. Johnson, and J. A. Swanson.** A role for phosphoinositide 3-kinase in the completion of macropinocytosis and phagocytosis by macrophages. *J. Cell Biol*. 135: 1249–1260, 1996.
4. **Backer, J. M., S. E. Shoelson, E. Haring, and M. F. White.** Insulin receptors internalize by a rapid, saturable pathway requiring receptor autophosphorylation and an intact juxtamembrane region. *J. Cell Biol*. 115: 1535–1545, 1991.
5. **Bar-Sagi, D., and J. R. Feramisco.** Induction of membrane ruffling and fluid-phase pinocytosis in quiescent fibroblasts by ras proteins. *Science* 233: 1061–1068, 1986.
6. **Birnbaum, M. J.** The insulin-sensitive glucose transporter. *Int. Rev. Cytol*. 137: 239–297, 1992.
7. **Cooper, A. D.** Hepatic uptake of chylomicron remnants. *J. Lipid Res*. 38: 2173–2192, 1997.
8. **Cox, A. D., P. A. Solski, J. D. Jordan, and C. J. Der.** Analysis of Ras protein expression in mammalian cells. *Methods Enzymol*. 255: 195–220, 1995.
9. **Crews, C. M., A. Alessandrini, and R. L. Erikson.** Erks: their fifteen minutes has arrived. *Cell Growth Differ*. 3: 135–142, 1992.
10. **Dudley, D. T., L. Pang, S. J. Decker, A. J. Bridges, and A. R. Saltiel.** A synthetic inhibitor of the mitogen-activated protein kinase cascade. *Proc. Natl. Acad. Sci. USA* 92: 7686–7689, 1995.
11. **Ebina, Y., L. Ellis, K. Jarnagin, M. Edery, L. Graf, E. Clauser, J. H. Ou, F. Masiarz, Y. W. Kan, I. D. Goldfine, R. A. Roth, and W. J. Rutter.** The human insulin receptor cDNA: the structural basis for hormone-activated transmembrane signalling. *Cell* 40: 747–758, 1985.
12. **Fraser, R., B. R. Dobbs, and G. W. Rogers.** Lipoproteins and the liver sieve: the role of the fenestrated sinusoidal endothelium in lipoprotein metabolism, atherosclerosis, and cirrhosis. *Hepatology* 21: 863–874, 1995.
13. **Gibbs, E. M., and G. E. Lienhard.** Fluid-phase endocytosis by isolated rat adipocytes. *J. Cell. Physiol*. 121: 569–575, 1984.
14. **Gibbs, E. M., G. E. Lienhard, J. R. Appleman, M. D. Lane, and S. C. Frost.** Insulin stimulates fluid-phase endocytosis and exocytosis in 3T3-L1 adipocytes. *J. Biol. Chem*. 261: 3944–3951, 1986.
15. **Harada, S., E. G. Loten, R. M. Smith, and L. Jarett.** Nonreceptor mediated nuclear accumulation of insulin in H35 rat hepatoma cells. *J. Cell. Physiol*. 153: 607–613, 1992.
16. **Harada, S., R. M. Smith, J. A. Smith, M. F. White, and L. Jarett.** Insulin-induced egr-1 and c-fos expression in 32D cells requires insulin receptor, Shc, and mitogen-activated protein kinase, but not insulin receptor substrate-1 and phosphatidylinositol 3-kinase activation. *J. Biol. Chem*. 271: 30222–30226, 1996.
17. **Janssen, K.** *Current Protocols in Molecular Biology*. New York: Wiley, 1993, vol. I, p. 9.1.3.
18. **Jess, T. J., C. M. Belham, F. J. Thomson, P. H. Scott, R. J. Plevin, and G. W. Gould.** Phosphatidylinositol 3′-kinase, but not p70 ribosomal S6 kinase, is involved in membrane protein recycling: wortmannin inhibits glucose transport and downregulates cell-surface transferrin receptor numbers independently of any effect on fluid-phase endocytosis in fibroblasts. *Cell. Signal*. 8: 297–304, 1996.
19. **Joneson, T., M. McDonough, D. Bar-Sagi, and L. Van Aelst.** RAC regulation of actin polymerization and proliferation by a pathway distinct from Jun kinase. *Science* 274: 1374–1376, 1996.
20. **Joneson, T., M. A. White, M. H. Wigler, and D. Bar-Sagi.** Stimulation of membrane ruffling and MAP kinase activation by distinct effectors of RAS. *Science* 271: 810–812, 1996.
21. **Kanai, F., K. Ito, M. Todaka, H. Hayashi, S. Kamohara, K. Ishii, T. Okada, O. Hazeki, M. Ui, and Y. Ebina.** Insulin-stimulated GLUT4 translocation is relevant to the phosphorylation of IRS-1 and the activity of PI3-kinase. *Biochem. Biophys. Res. Commun*. 195: 762–768, 1993.
22. **Kapeller, R., and L. C. Cantley.** Phosphatidylinositol 3-kinase. *Bioessays* 16: 565–576, 1994.

23. **Kotani, K., K. Hara, K. Kotani, K. Yonezawa, and M. Kasuga.** Phosphoinositide 3-kinase as an upstream regulator of the small GTP-binding protein Rac in the insulin signaling of membrane ruffling. *Biochem. Biophys. Res. Commun*. 208: 985–990, 1995.
24. **Kotani, K., K. Yonezawa, K. Hara, H. Ueda, Y. Kitamura, H. Sakaue, A. Ando, A. Chavanieu, B. Calas, F. Grigorescu, M. Nishiyama, M. D. Waterfield, and M. Kasuga.** Involvement of phosphoinositide 3-kinase in insulin- or IGF-1-induced membrane ruffling. *EMBO J*. 13: 2313–2321, 1994.
25. **Lewis, W. H.** Pinocytosis. *Bull. Johns Hopkins Hosp*. 49: 17–36, 1931.
26. **Li, S. L., Y. Miyata, I. Yahara, and Y. Fujita-Yamaguchi.** Insulin-induced circular membrane ruffling on rat 1 cells expressing a high number of human insulin receptors: circular ruffles caused by rapid actin reorganization exhibit high density of insulin receptors and phosphotyrosines. *Exp. Cell Res*. 205: 353–360, 1993.
27. **Livingston, J. N., B. R. Saran, C. D. Rose, and C. L. Anderson.** Rapid effects of insulin on the cycling of the insulin receptor in a human monocyte cell line (U-937). *Diabetes* 34: 403–408, 1985.
28. **Maegawa, H., D. A. McClain, G. Freidenberg, J. M. Olefsky, M. Napier, T. Lipari, T. J. Dull, J. Lee, and A. Ullrich.** Properties of a human insulin receptor with a COOH-terminal truncation. II. Truncated receptors have normal kinase activity but are defective in signaling metabolic effects. *J. Biol. Chem*. 263: 8912–8917, 1988.
29. **Maegawa, H., J. M. Olefsky, S. Thies, D. Boyd, A. Ullrich, and D. A. McClain.** Insulin receptors with defective tyrosine kinase inhibit normal receptor function at the level of substrate phosphorylation. *J. Biol. Chem*. 263: 12629–12637, 1988.
30. **McClain, D. A., H. Maegawa, J. Lee, T. J. Dull, A. Ulrich, and J. M. Olefsky.** A mutant insulin receptor with defective tyrosine kinase displays no biologic activity and does not undergo endocytosis. *J. Biol. Chem*. 262: 14663–14671, 1987.
31. **McClain, D. A., H. Maegawa, J. Levy, T. Huecksteadt, T. J. Dull, J. Lee, A. Ullrich, and J. M. Olefsky.** Properties of a human insulin receptor with a COOH-terminal truncation. I. Insulin binding, autophosphorylation, and endocytosis. *J. Biol. Chem*. 263: 8904–8911, 1988.
32. **McClain, D. A., H. Maegawa, R. S. Thies, and J. M. Olefsky.** Dissection of the growth versus metabolic effects of insulin and insulin-like growth factor-I in transfected cells expressing kinase-defective human insulin receptors. *J. Biol. Chem*. 265: 1678–1682, 1990.
33. **Miyata, Y., M. Hoshi, S. Koyasu, T. Kadowaki, M. Kasuga, I. Yahara, E. Nishida, and H. Sakai.** Rapid stimulation of fluid-phase endocytosis and exocytosis by insulin, insulin-like growth factor-I, and epidermal growth factor in KB cells. *Exp. Cell Res*. 178: 73–83, 1988.
34. **Morrill, G. A., A. B. Kostellow, and S. P. Weinstein.** Endocytosis in the amphibian oocyte. Effect of insulin and progesterone on membrane and fluid internalization during the meiotic divisions. *Biochim. Biophys. Acta* 803: 71–77, 1984.
35. **Moss, A. L., and W. F. Ward.** Multiple pathways for ligand internalization in rat hepatocytes. I: Effects of anoxia, phenylarsine oxide and monensin. *J. Cell. Physiol*. 149: 313–318, 1991.
36. **Myers, M. G., Jr., and M. F. White.** Insulin signal transduction and the IRS proteins. *Annu. Rev. Pharmacol. Toxicol*. 36: 615–658, 1996.
37. **Nakanishi, S., S. Kakita, I. Takahashi, K. Kawahara, E. Tsukuda, T. Sano, K. Yamada, M. Yoshida, H. Kase, Y. Matsuda, Y. Hashimoto, and Y. Nonomura.** Wortmannin, a microbial product inhibitor of myosin light chain kinase. *J. Biol. Chem*. 267: 2157–2163, 1992.
38. **Oefelein, M. G., G. Arsenis, and J. N. Livingston.** Insulin-stimulated fluid-phase pinocytosis and internalization of the insulin receptor: differences between the U-937 monocyte and rat adipocyte. *Metabolism* 35: 818–823, 1986.
39. **Oliver, J. M., R. D. Berlin, and B. H. Davis.** Use of horseradish peroxidase and fluorescent dextrans to study fluid pinocytosis in leukocytes. *Methods Enzymol*. 108: 336–347, 1984.
40. **Quilliam, L. A., K. Kato, K. M. Rabun, M. M. Hisaka, S. Y. Huff, S. Campbell-Burk, and C. J. Der.** Identification of residues critical for Ras(17N) growth-inhibitory phenotype and for Ras interaction with guanine nucleotide exchange factors. *Mol. Cell. Biol*. 14: 1113–1121, 1994.
41. **Quon, M. J., A. J. Butte, M. J. Zarnowski, G. Sesti, S. W. Cushman, and S. I. Taylor.** Insulin receptor substrate 1 mediates the stimulatory effect of insulin on GLUT4 translocation in transfected rat adipose cells. *J. Biol. Chem*. 269: 27920–27924, 1994.
42. **Ridley, A. J.** Membrane ruffling and signal transduction. *Bioessays* 16: 321–327, 1994.
43. **Robinson, M. S., C. Watts, and M. Zerial.** Membrane dynamics in endocytosis. *Cell* 84: 13–21, 1996.
44. **Ruderman, N. B., R. Kapeller, M. F. White, and L. C. Cantley.** Activation of phosphatidylinositol 3-kinase by insulin. *Proc. Natl. Acad. Sci. USA* 87: 1411–1415, 1990.
45. **Saltiel, A. R.** Diverse signaling pathways in the cellular actions of insulin. *Am. J. Physiol*. 270 (*Endocrinol. Metab*. 33): E375–E385, 1996.
46. **Scherer, P. E., M. P. Lisanti, G. Baldini, M. Sargiacomo, C. C. Mastick, and H. F. Lodish.** Induction of caveolin during adipogenesis and association of GLUT4 with caveolin-rich vesicles. *J. Cell Biol*. 127: 1233–1243, 1994.
47. **Schlessinger, J., and D. Bar-Sagi.** Activation of Ras and other signaling pathways by receptor tyrosine kinases. *Cold Spring Harb. Symp. Quant. Biol*. 59: 173–179, 1994.
48. **Storrie, B., and E. A. Madden.** Isolation of subcellular organelles. *Methods Enzymol*. 182: 203–225, 1990.
49. **Stossel, T. P.** On the crawling of animal cells. *Science* 260: 1086–1094, 1993.
50. **Stumpo, D. J., and P. J. Blackshear.** Cellular expression of mutant insulin receptors interferes with the rapid transcriptional response to both insulin and insulin-like growth factor I. *J. Biol. Chem*. 266: 455–460, 1991.
51. **Thies, R. S., A. Ullrich, and D. A. McClain.** Augmented mitogenesis and impaired metabolic signaling mediated by a truncated insulin receptor. *J. Biol. Chem*. 264: 12820–12825, 1989.
52. **Ui, M., T. Okada, K. Hazeki, and O. Hazeki.** Wortmannin as a unique probe for an intracellular signalling protein, phosphoinositide 3-kinase. *Trends Biochem. Sci*. 20: 303–307, 1995.
53. **Van der Geer, P., T. Hunter, and R. A. Lindberg.** Receptor protein-tyrosine kinases and their signal transduction pathways. *Annu. Rev. Cell Biol*. 10: 251–337, 1994.
54. **Wang, L. M., M. G. Myers, Jr., X. J. Sun, S. A. Aaronson, M. White, and J. H. Pierce.** IRS-1: essential for insulin- and IL-4-stimulated mitogenesis in hematopoietic cells. *Science* 261: 1591–1594, 1993.
55. **West, M. A., M. S. Bretscher, and C. Watts.** Distinct endocytotic pathways in epidermal growth factor-stimulated human carcinoma A431 cells. *J. Cell Biol*. 109: 2731–2739, 1989 [published erratum appears in *J. Cell Biol*. 110: 859, 1990].
56. **White, M. F., and C. R. Kahn.** The insulin signaling system. *J. Biol. Chem*. 269: 1–4, 1994.
57. **Wiley, H. S., and D. D. Cunningham.** Epidermal growth factor stimulates fluid phase endocytosis in human fibroblasts through a signal generated at the cell surface. *J. Cell. Biochem*. 19: 383–394, 1982.
58. **Wiley, H. S., and D. N. McKinley.** Assay of growth factor stimulation of fluid-phase endocytosis. *Methods Enzymol*. 146: 402–417, 1987.
59. **Wiley, H. S., B. J. Walsh, and K. A. Lund.** Global modulation of the epidermal growth factor receptor is triggered by occupancy of only a few receptors. Evidence for a binary regulatory system in normal human fibroblasts. *J. Biol. Chem*. 264: 18912–18920, 1989.
60. **Xu, G., J. Howland, and P. L. Rothenberg.** Insulin and secretagogues differentially regulate fluid-phase pinocytosis in insulin-secreting beta-cells. *Biochem. J*. 318: 623–629, 1996.